Article

Discovery Medicine 2026; 38(210): 2252–2259
https://doi.org/10.24976/Discov.Med.202638210.176

Knockdown of IGFBP7 Alleviates High Glucose-Triggered Vascular Endothelial Injury and Is Associated With the Upregulation of AURKA in HUVECs

Zhao Liu[1], Bin Liu[1], Liwei Zhang[1], Hai Feng[1,*]

[1]Department of Vascular Surgery, Beijing Friendship Hospital, Capital Medical University, 100050 Beijing, China
*Correspondence: fenghaichina@163.com (Hai Feng)
Submitted: 8 June 2026 Revised: 24 June 2026 Accepted: 10 July 2026 Published: 23 July 2026

Background: Progressive vascular endothelial cell (EC) injury is a key initiating event in diabetic macrovascular complications, which dramatically increases morbidity and mortality among diabetic patients by facilitating atherosclerotic lesion formation and subsequent cardio-cerebrovascular disorders. Chronic hyperglycaemia impairs endothelial proliferation, migration and angiogenic capacity; however, the key molecules regulating high glucose (HG)-mediated endothelial deterioration remain incompletely characterized. This study aimed to uncover the molecular cascade underlying HG-triggered human endothelial damage.

Methods: Human umbilical vein endothelial cells (HUVECs) were randomly divided into multiple groups and incubated in medium supplemented with either physiological isotonic glucose or HG to construct an *in vitro* endothelial injury model induced by hyperglycaemia. Synthetic small interfering RNAs (siRNAs) were transiently transfected into HUVECs via liposomal delivery to achieve specific knockdown of insulin-like growth factor-binding protein 7 (IGFBP7) and aurora kinase A (AURKA) separately or simultaneously, with scrambled siRNA serving as the negative transfection control. After completion of drug and gene intervention, multiple sets of functional indicators (viability, migration, tube formation) and apoptotic-related molecular signatures (B-cell lymphoma 2 (Bcl-2), BCL2-associated X, apoptosis regulator (Bax), and Cleaved Caspase-3) were systematically measured to comprehensively evaluate the severity of endothelial injury.

Results: HG exposure significantly impaired the fundamental biological behaviours of HUVECs, while simultaneously elevating IGFBP7 expression, depressing AURKA transcription, and tipping the equilibrium of apoptosis-related proteins: Bcl-2, Bax and Cleaved Caspase-3 ($p < 0.05$). Silencing IGFBP7 remarkably rescued HG-induced endothelial dysfunction, yet AURKA knockdown partly reversed these protective phenotypes ($p < 0.05$).

Conclusion: IGFBP7 knockdown alleviates HG-induced endothelial injury, and this effect may be associated with upregulation of AURKA. These findings provide preliminary experimental evidence supporting further investigation of potential therapeutic targets for diabetic vascular complications.

Keywords: high glucose; vascular endothelial cell injury; insulin-like growth factor-binding protein 7; aurora kinase A; diabetic vascular complication

Introduction

Diabetes mellitus (DM) has become an epidemic chronic disease worldwide; by 2045, the prevalence of DM among individuals aged 20–79 is forecast to reach 12.2% (783.2 million people) [1]. Diabetic vascular complications, which occur in microvessels and macrovessels, are the most important cause of morbidity and mortality in the DM population [2]. Therein, atherosclerosis emerges as a major macrovascular complication and a leading cause of cardiovascular disease (CVD), imposing a substantial burden on survival outcomes in patients with DM [3]. Hence, studying the mechanisms underlying macrovascular complications in DM may provide important insights for improving patient survival.

Endothelial cells (ECs) and their products NO and prostacyclin are essential for the maintenance of vascular homeostasis [4]. Disturbed glucose metabolism and hyperglycemia-induced oxidative stress and inflammatory responses contribute to vascular EC injury and subsequent endothelial dysfunction, which represents a key pathogenic mechanism in diabetic vascular complications [5,6]. Damaged ECs primarily exhibit impaired barrier function, reduced migration and proliferation, impaired diastolic function, increased apoptosis, and most importantly, compromised angiogenic capacity [2,7,8]. Although the mechanism of EC injury in DM has been explored in recent years, the findings remain inconclusive.

Insulin-like growth factor-binding protein 7 (IGFBP7), a secretory protein, can exert either positive or adverse effects on IGF signaling due to its strong affinity for IGF binding. In an IGF-independent manner, it is also essential for cell proliferation, differentiation, and development [9]. The interaction between IGFBP7 and IGFs has been implicated in the progression of DM [10]. Furthermore, IGFBP7 has been suggested to play a role in diabetic vascular complications [11]; however, its underlying mechanism remains unclear. Notably, transcriptome analysis has revealed that IGFBP7 is upregulated in damaged ECs [12]. Accordingly, IGFBP7 may contribute to the injury of ECs in DM.

Aurora kinase A (AURKA), one of the three members of the aurora kinase family, is responsible for regulating multiple processes during cell caryomitosis, including microtubule stability in the G1 phase, as well as chromosomal segregation and alignment [13]. To date, AURKA has been recognized as an oncogene in multiple cancer types, and targeting AURKA has been shown to suppress cancer progression and drug resistance [14,15]. Additionally, a recent study suggested that AURKA promotes post-ischemic angiogenesis in diabetic limb ischemia [16]. Notably, a protective role of AURKA in ECs exposed to high glucose (HG) has also been reported [16]. Therefore, AURKA is likely involved in endothelial injury in DM.

Here, we speculated that there is a relationship between IGFBP7 and AURKA and investigated their roles in EC injury in DM using *in vitro* loss-of-function experiments in HG-induced ECs.

Materials and Methods

Cell Culture and Transfection

Human umbilical vein ECs (HUVECs, PCS-100-013) were obtained from the American Type Culture Collection (Manassas, VA, USA) and cultured in 96-well plates using complete Roswell Park Memorial Institute (RPMI)-1640 medium (PM150110B, Procell, Wuhan, China). The cell line tested negative for mycoplasma contamination and was confirmed to have accurate short tandem repeat profiling. Plates were maintained at 37 °C and 5% CO_2 in an incubator (51032874, ThermoFisher Scientific, Waltham, MA, USA).

The small interfering RNA against IGFBP7 (siIGFBP7, siG000003490A-1-5, sense strand: 5′-CAAUCCACUAACACUUUAGUU-3′; antisense strand: 5′-ACUAAAGUGUUAGUGGAUUG-3′), siAURKA (siB14210102904-1-5, sense strand: 5’-CCUGUCUUACUGUCAUUCGAA-3’; antisense strand: 5′-UUCGAUGACAGUAAGACAGG-3′), and scrambled siRNA negative control (siNC, siN0000002-1-5, sense strand: 5′-UUCUCCGAACGUGUCACGUUU-3′; antisense strand: 5′-ACGUGACACGUUCGGAGAAUU-3′) were all obtained from RIBOBIO (Guangzhou, China). For cell transfection, HUVECs were seeded into 96-well plates at a density of 1×10^4 cells/well. Transfection was conducted when cell confluence reached 70%–90%. All siRNAs (siIGFBP7, siAURKA and siNC) were diluted to a final working concentration of 50 nM before complex preparation. Liposome–siRNA complexes were formulated following the manufacturer’s instructions for the Lipofectamine 3000 Transfection Reagent (L3000001, ThermoFisher Scientific, Waltham, MA, USA). Cells were cultured at 37 °C for 48 hours (h) after transfection, and quantitative reverse transcriptase polymerase chain reaction (qRT-PCR) was performed to detect the target gene knockdown efficiency.

Cell Treatment

After cell passage, HUVECs were cultured in complete RPMI-1640 medium supplemented with 30 mmol/L glucose (G7021, Sigma-Aldrich, St. Louis, MO, USA) for 48 h [17]. In parallel, control cells were cultured in control glucose medium (5 mmol/L glucose and 25 mmol/L mannitol). Mannitol (M4125) was purchased from Sigma-Aldrich (St. Louis, MO, USA).

Cell Counting Kit-8 (CCK-8) Assay

After the cells had been treated for 24 or 48 h, WST-8/CCK-8 Solution (10 µL/well) in Cell Counting Kit-8 (ab228554, Abcam, Cambridge, UK) was added to each well for a 4-h incubation period at 37 °C without light. The optical density (OD) value of each well at 0, 24 and 48 h were measured at 460 nm using the Multiskan™ FC enzyme-labeled instrument (ThermoFisher Scientific, Waltham, MA, USA).

Scratch Assay

6-well plates were seeded with 5×10^5 HUVECs per well. Once the monolayers reached 90%–100% confluence, cells were cultured in serum-free media, rinsed three times with phosphate-buffered saline (PBS, abs962, Absin, Shanghai, China), and scratched with sterile pipette tips. Floating detached cells were removed by gentle PBS washing again after scratching. An Olympus BX53F microscope (100×, OLYMPUS, Tokyo, Japan) was used to capture wound images at 0 and 48 h, and ImageJ (v1.52s, National Institutes of Health, Bethesda, MD, USA) was used to quantify the images.

Tube Formation Assay

Firstly, 50 µL/well Matrigel homogenate (356234, Solarbio, Beijing, China) was pre-coated on the 24-well plates. Afterwards, HUVECs were cultured on the Matrigel with a density of 1.5×10^4 cells/well for 3–12 h. Finally, HUVECs were fixed with 4% paraformaldehyde (abs9179, Absin, Shanghai, China), and the BX53F microscope was used to observe the formed tubes at 100× magnification, followed by analysis using ImageJ software (v1.52s, National Institutes of Health, Bethesda, MD, USA).

qRT-PCR

The first-strand complementary DNA (cDNA) was synthesized using the SuperScriptTM VILOTM cDNA Synthesis Kit (11754050, ThermoFisher Scientific, Waltham, MA, USA) following the extraction of the total RNA of HUVECs using the TRIzolTM Plus RNA Purification Kit (12183555, ThermoFisher Scientific, Waltham, MA, USA). Then, the synthesized cDNA was used for qRT-PCR with Fast SYBR™ Green Master Mix (4385612, ThermoFisher Scientific, Waltham, MA, USA) on a QuantStudio™ 7 Pro real-time PCR instrument (A43165, ThermoFisher Scientific, Waltham, MA, USA), under the following conditions: 95 °C for 20 sec, followed by 40 cycles of 95 °C for 3 sec and 60 °C for 30 sec. Finally, β-actin was used as the internal control, and all data were analyzed using the $2^{-\Delta\Delta CT}$ method [18].

The primers used are listed as follows: IGFBP7 primers, sense: 5′-GAAGTAACTGGCTGGGTGCT-3′, antisense: 5′-ATGCCCTTATGGGTTGCTAACT-3′; AURKA primers, sense: 5′-GTCAAGTCCCCTGTCGGTTC-3′, antisense: 5′-GGCAATGGAGTGAGACCCTC-3′; β-actin primers, sense: 5′-CAAATGCTTCTAGGCGGACTATG-3′, antisense: 5′-TGCGCAAGTTAGGTTTTGTCA-3′.

Western Blotting

RIPA lysis buffer (R0010, Solarbio, Beijing, China) was used to extract total cellular protein from HUVECs. The BCA Protein Assay Kit (PC0020, Solarbio, Beijing, China) was used to measure the total protein content after protein samples were denatured in a boiling water bath for five minutes. Sodium dodecyl sulfate-polyacrylamide gel electrophoresis (SDS-PAGE) was used to separate equal amounts of denatured protein on 10% separating gels (XP00100BOX, ThermoFisher Scientific, Waltham, MA, USA). Subsequently, separated proteins were electrophoretically transferred onto Immobilon-P PVDF membranes (E801-01, Vazyme, Vazyme, China). After blocking membranes for 1 h at room temperature using Blocking Buffer (37581, ThermoFisher Scientific, Waltham, MA, USA), the membranes were incubated with primary antibodies overnight at 4 °C, and then incubated for 1 h at room temperature with matching secondary antibodies. A Tanon 5200 imaging system (Tanon, Shanghai, China) was used to visualize protein bands following chemiluminescent detection. ImageJ software was utilized to quantify relative band intensities, while β-actin served as the internal reference for normalization.

The antibodies used are as follows: primary antibodies included B-cell lymphoma 2 (Bcl-2, ab59348, 26 kDa, 1:500, Abcam, Cambridge, UK), BCL2 associated X, apoptosis regulator (Bax, ab32503, 21 kDa, 1:2000, Abcam, Cambridge, UK), Cleaved Caspase-3 (ab2302, 17 kDa, 1:2000, Abcam, Cambridge, UK), AURKA (#14475, 48 kDa, 1:1000, Cell Signaling Technology, Danvers, MA, USA) and β-actin (ab8227, 42 kDa, 1:1000, Abcam, Cambridge, UK), and secondary antibodies included anti-rabbit IgG (ab205718, 1:2000, Abcam, Cambridge, UK).

Statistical Analyses

The study data were obtained from three independent experiments, and GraphPad Prism 8 (GraphPad, Inc., USA) was used to express the results as mean ± standard deviation. The comparison between two groups was conducted using an independent samples *t*-test, and the comparison among multiple groups was performed using a one-way analysis of variance (ANOVA). Statistical significance was defined as a *p*-value less than 0.05.

Results

HG Exposure Inhibited Cell Viability and Upregulated IGFBP7 Expression in HUVECs

To mimic the HG environment to which ECs are exposed in DM, HG medium was used to culture HUVECs *in vitro*. As shown, cell viability at 24 and 48 h in the HG group was decreased compared with the Control group (Fig. 1A, $p < 0.01$). Also, data from qRT-PCR demonstrated the upregulated expression of IGFBP7 at 24 h and 48 h following HG exposure (Fig. 1B, $p < 0.001$).

IGFBP7 Deletion Accelerated Viability, Migration, and Tube Formation of HUVECs With HG Exposure

We demonstrated that IGFBP7 expression is increased in HUVECs exposed to HG. Furthermore, IGFBP7 was deleted in HUVECs by siIGFBP7 transfection to investigate its role (Fig. 2A, $p < 0.001$). Cell viability, migration, and tube formation were significantly reduced in the HG group compared with the Control group (Fig. 2B–F, $p < 0.01$). Moreover, in HG-induced HUVECs transfected with siIGFBP7, cell viability, migration, and tube formation were significantly increased compared with the HUVECs containing siNC (Fig. 2B–F, $p < 0.05$). These data suggest that IGFBP7 deletion restores the decreased viability, migration, and tube formation in HG-induced HUVECs.

AURKA Deletion Reversed the Effects of IGFBP7 Deletion in HUVECs Exposed to HG

Additionally, AURKA expression was reduced in HUVECs following HG exposure (Fig. 2G, $p < 0.001$). Compared with HG-induced HUVECs transfected with siNC, AURKA expression was significantly higher in cells transfected with siIGFBP7 (Fig. 2G, $p < 0.01$), suggesting a potential regulation of IGFBP7 on AURKA. To further investigate the role of the IGFBP7/AURKA axis in HG-induced EC injury, AURKA was silenced using siAURKA transfection. AURKA expression was significantly reduced in the HG+siAURKA group compared with the HG+siNC group (Fig. 2H,I, $p < 0.01$). Furthermore, siAURKA reversed

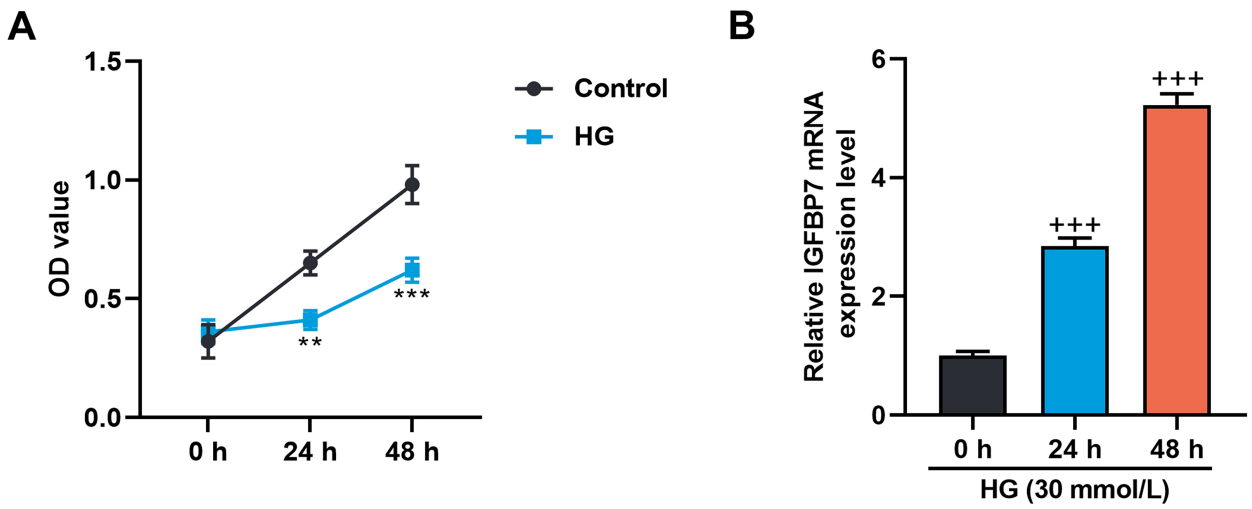

Fig. 1. Effects of high glucose (HG) exposure on cell viability and insulin-like growth factor-binding protein 7 (IGFBP7) expression in human umbilical vein endothelial cells (HUVECs). (A,B) After HUVECs were exposed to HG environment (30 mmol/L glucose), with control cells cultured in a medium containing 5 mmol/L glucose and 25 mmol/L mannitol, cell viability at 0 h, 24 h and 48 h was assessed using a cell counting kit-8 (CCK-8) assay (OD, optical density) (A), and quantitative reverse transcriptase polymerase chain reaction (qRT-PCR) was used to evaluate IGFBP7 expression in HUVECs at 0 h, 24 h, and 48 h, with β-actin as the internal reference (B). Data are presented as mean ± SD (three independent repeated experiments). $^{**}p < 0.01$; $^{***}p < 0.001$ vs. Control; $^{+++}p < 0.001$ vs. 0 h.

the effect of siIGFBP7 on the expression of AURKA (Fig. 3A, $p < 0.05$). Then, it was found that siAURKA inhibited cell viability, migration, and tube formation in HG-induced HUVECs compared with the HG+siNC group (Fig. 3B–F, $p < 0.01$). Moreover, the promotive effects of IGFBP7-deletion on the above indicators in HUVECs were partially reversed by further transfection with siAURKA (Fig. 3B–F, $p < 0.001$). To assess cell apoptosis, the expression of associated proteins was determined, including pro-apoptosis proteins Bax and Cleaved Caspase-3, and anti-apoptosis protein Bcl-2. HG exposure promoted cell apoptosis in HUVECs, as indicated by downregulated Bcl-2 expression and upregulated expression of Bax and Cleaved Caspase-3 following HG incubation (Fig. 4A,B, $p < 0.001$). In HG-exposed HUVECs, siIGFBP7 increased Bcl-2 expression while decreasing Bax and Cleaved Caspase-3 expression (Fig. 4A,B, $p < 0.01$), whereas siAURKA produced the opposite effects (Fig. 4A,B, $p < 0.05$). Moreover, siAURKA neutralized the inhibitory effects of siIGFBP7 on apoptosis in HG-exposed HUVECs (Fig. 4A,B, $p < 0.05$). These results indicate that AURKA deletion attenuates the effects of IGFBP7 deletion on HG-induced changes in viability, migration, tube formation, and apoptosis in HUVECs, suggesting that IGFBP7 may regulate EC injury in HG conditions through AURKA.

Discussion

CVD and cancer are the two leading causes of death in most countries, and it is well known that patients with DM have a substantially higher risk of CVD than healthy individuals, which is the major cause of death in patients with DM [19]. This is because the blood environment in DM is unfavorable for vascular homeostasis, thereby contributing to diabetic vascular complications such as atherosclerosis, a major cause of CVD [20]. It has also been recognized that EC injury is a key pathological event in diabetic vascular complications [21]. Hence, exploring the mechanism of endothelial injury induced by HG may provide important insights into the treatment of diabetic vascular complications. In this study, we found that IGFBP7 expression was upregulated, whereas AURKA expression was downregulated in HG-induced HUVECs, and IGFBP7 deletion enhanced viability, migration, and tube formation of these cells, whereas this effect was attenuated by AURKA deletion. Based on these findings, we propose that IGFBP7 deletion is associated with AURKA upregulation, which may contribute to the observed protective effects.

As described above, integrated transcriptome analysis of ECs from traumatic brain tissues revealed IGFBP7 overexpression [12]. Here, we demonstrated that increased IGFBP7 expression was accompanied by decreased HUVEC viability following HG exposure, suggesting the involvement of IGFBP7 in HG-induced EC injury. Although previous studies have shown that IGFBP7 treatment inhibits

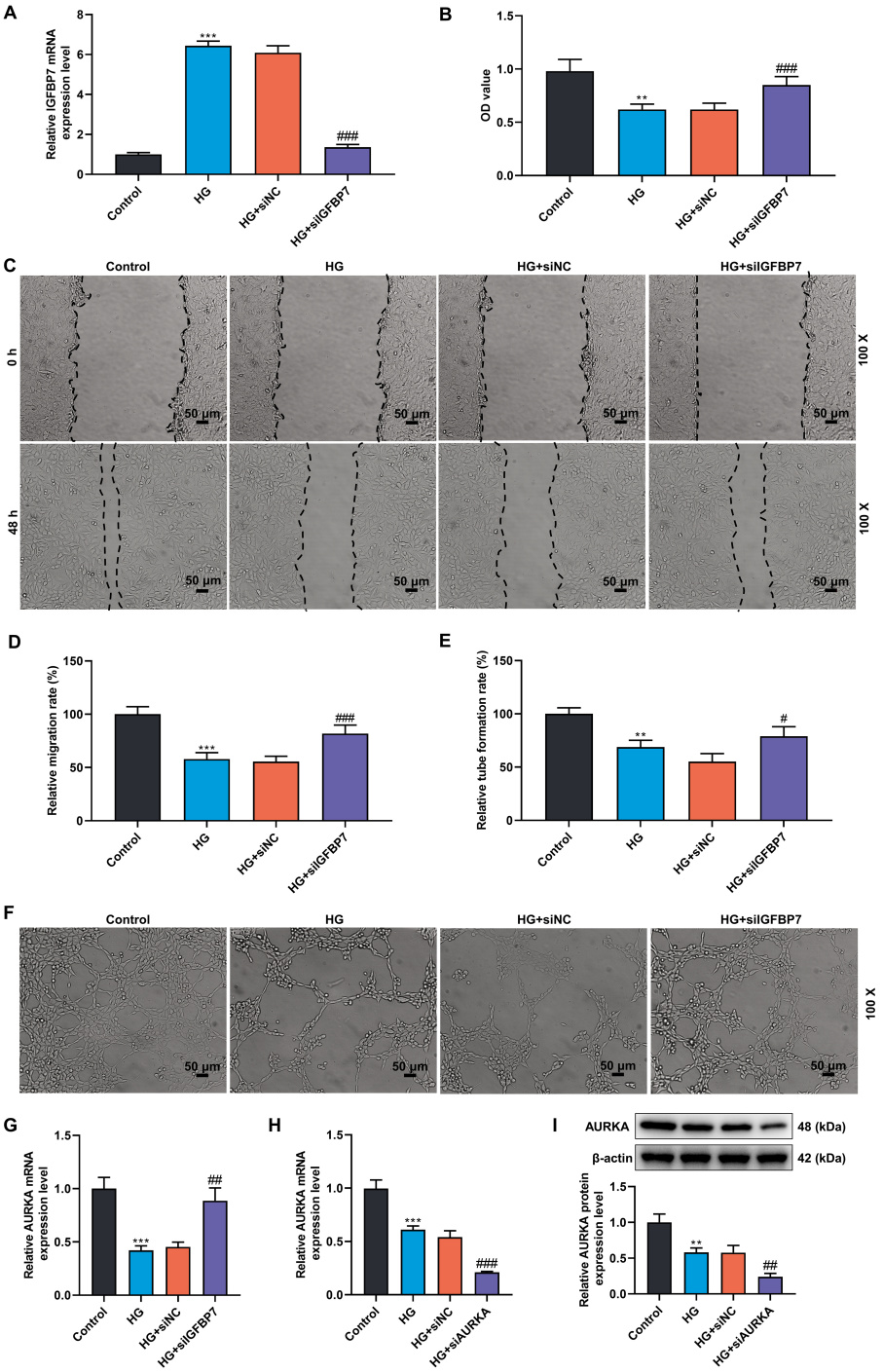

Fig. 2. Effect of IGFBP7 deletion on viability, migration, and tube formation in HUVECs with HG exposure. (A–G) After HUVECs were transfected with negative control small interfering RNA (siNC) or siIGFBP7, followed by HG exposure (Control, HG, HG+siNC, HG+siIGFBP7), qRT-PCR showed transfection efficiency, with β-actin as the internal reference (A), CCK-8 assay was utilized for viability determination (B), cell migration was measured with scratch assay (C,D, magnification: 100×; scale: 50 μm), *in vitro* tube formation was detected (E,F, magnification: 100×; scale: 50 μm), and aurora kinase A (AURKA) expression in HUVECs was determined by qRT-PCR, with β-actin as the internal reference (G). (H,I) After HUVECs were transfected with siNC or siAURKA, the AURKA expression in HUVECs was determined by qRT-PCR and Western blotting, with β-actin as the internal reference. Data are presented as mean ± SD (three independent repeated experiments). $^{**}p < 0.01$, $^{***}p < 0.001$ vs. Control; $^{\#}p < 0.05$, $^{\#\#}p < 0.01$, $^{\#\#\#}p < 0.001$ vs. HG+siNC.

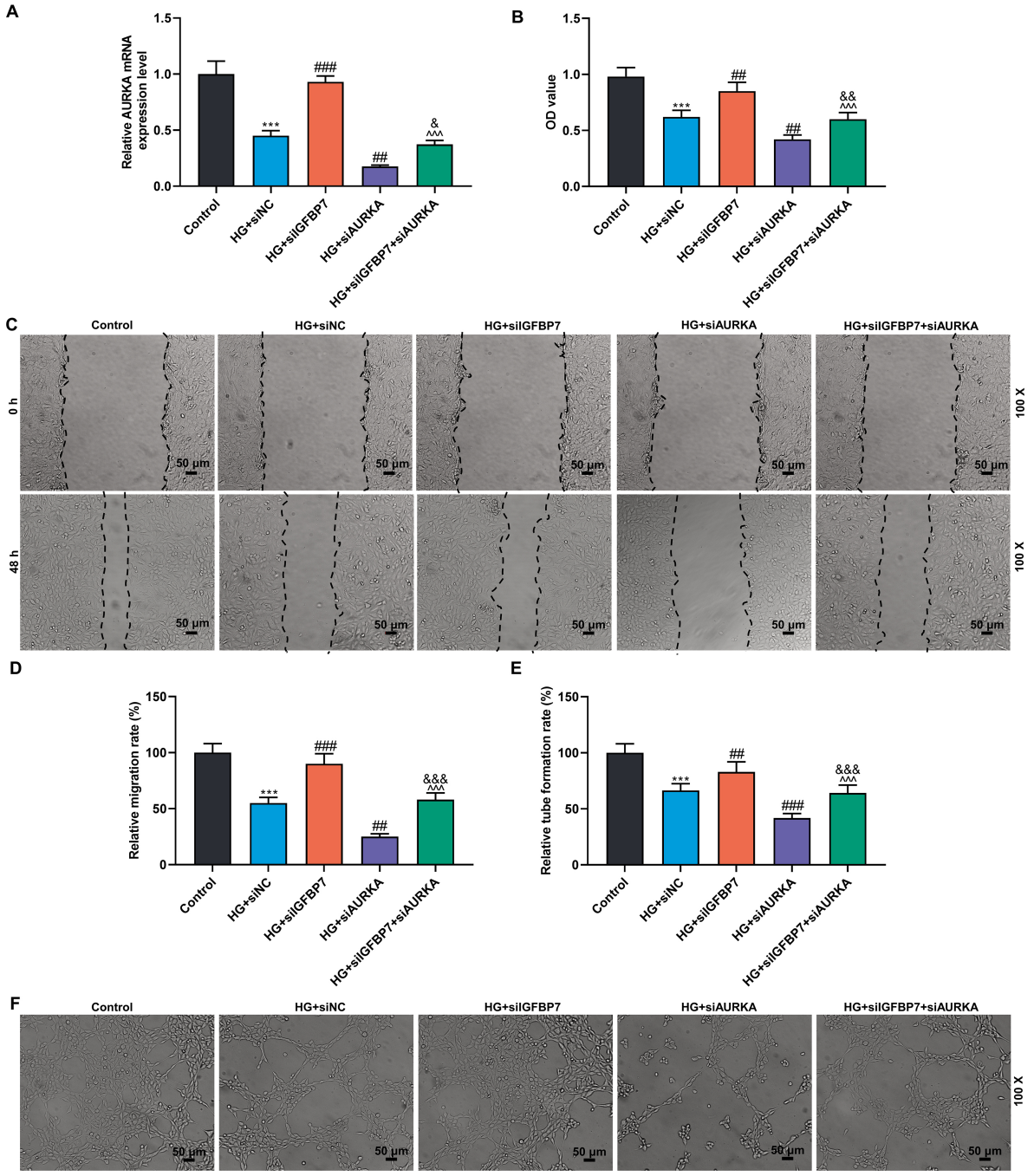

Fig. 3. Effect of AURKA deletion on viability, migration, and tube formation in HUVECs exposed to HG. (A–F) After HUVECs were transfected with siNC, siAURKA or/and siIGFBP7, followed by HG exposure (Control, HG+siNC, HG+siIGFBP7, HG+siAURKA, HG+siIGFBP7+siAURKA), qRT-PCR showed transfection efficiency, with β-actin as the internal reference (A), CCK-8 assay was utilized for viability determination (B), cell migration was measured with scratch assay (C,D, magnification: 100×; scale: 50 μm), and *in vitro* tube formation was detected (E,F, magnification: 100×; scale: 50 μm). Data are presented as mean ± SD (three independent repeated experiments). $^{***}p < 0.001$ vs. Control; $^{\#\#}p < 0.01$, $^{\#\#\#}p < 0.001$ vs. HG+siNC; $^{\wedge\wedge\wedge}p < 0.001$ vs. HG+siIGFBP7; $^{\&}p < 0.05$, $^{\&\&}p < 0.01$, $^{\&\&\&}p < 0.001$ vs. HG+siAURKA.

vascular endothelial growth factor (VEGF)-induced proliferation in HUVECs [22], its role in HG-induced EC injury remains unclear. In this study, IGFBP7 deletion reversed HG-induced reductions in HUVEC viability, migration and tube formation, as well as increased apoptosis. Notably, tube formation is critical for vascularization *in vivo*, in which the proliferation and migration of ECs play essential roles [23]. These findings indicate that HG induces in-

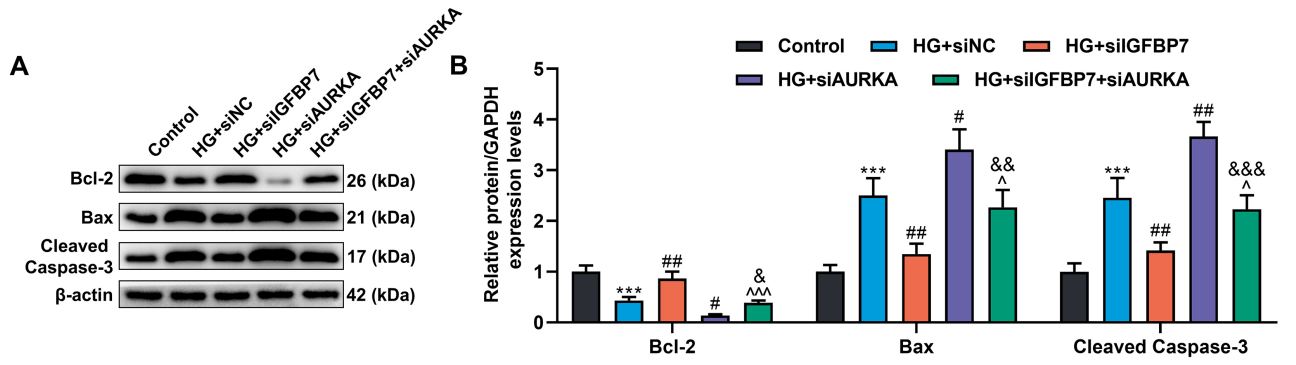

Fig. 4. Effect of IGFBP7 and AURKA deletion on apoptosis-associated protein expression in HUVECs exposed to HG. (A,B) Western blotting exhibited expression of apoptosis-associated proteins (Bcl-2, Bax, Cleaved Caspase-3) in HUVECs in the Control, HG+siNC, HG+siIGFBP7, HG+siAURKA, HG+siIGFBP7+siAURKA groups, with β-actin as the internal reference. Data are presented as mean ± SD (three independent repeated experiments). $^{***}p < 0.001$ vs. Control; $^{\#}p < 0.05$, $^{\#\#}p < 0.01$ vs. HG+siNC; $^{\wedge}p < 0.05$, $^{\wedge\wedge\wedge}p < 0.001$ vs. HG+siIGFBP7; $^{\&}p < 0.05$, $^{\&\&}p < 0.01$, $^{\&\&\&}p < 0.001$ vs. HG+siAURKA.

jury of HUVECs, whereas IGFBP7 deletion alleviates these effects. We also noted that HG promotes proliferation, migration, and tube formation in retinal endothelial cells, contributing to neovascularization in retinal tissues and diabetic retinopathy [24]. Thus, the effects of HG on ECs differ between diabetic macrovascular and microvascular complications. Overall, our in vitro cellular findings suggest that targeted inhibition of IGFBP7 may serve as a potential protective strategy against high glucose-triggered HUVECs damage.

In exploring the mechanism of IGFBP7, AURKA attracted our attention. A recent study reported that AURKA rescues cell cycle progression, proliferation, migration, and tube formation in HG-damaged ECs by inhibiting ferroptosis [16]. Consistently, our study found that AURKA deletion inhibited viability, migration, and tube formation, while promoting apoptosis in HG-induced HUVECs, indicating its essential role in maintaining EC function. Although a direct link between IGFBP7 and AURKA has not been reported, our data showed a negative correlation between their expression in HG-stimulated HUVECs. Moreover, AURKA knockdown reversed the protective effects of IGFBP7 silencing on HG-induced endothelial injury. These phenotypic results suggest that AURKA may act as a functional downstream molecule mediating the biological effects of IGFBP7 in HG-induced endothelial injury.

It should be emphasized that the current study only suggested an expression correlation and functional epistasis between IGFBP7 and AURKA. The precise molecular mechanism by which IGFBP7 regulates AURKA remains unclear. Collectively, these findings indicate a combined role of IGFBP7 and AURKA in HG-mediated endothelial damage, and provide a preliminary basis for identifying potential therapeutic targets for diabetic macrovascular complications.

Conclusion

To sum up, this study demonstrates that knockdown of IGFBP7 correlates with AURKA upregulation and alleviates HG-induced endothelial injury in HUVECs. We hypothesize that IGFBP7 and AURKA may antagonistically influence EC function under high-glucose conditions. However, direct mechanistic evidence is still lacking, and all findings are currently limited to *in vitro* experiments. Therefore, although this study provides a preliminary basis for further investigation, the translational potential of targeting IGFBP7 or AURKA in diabetic macrovascular complications requires further *in vivo* validation and mechanistic studies.

Availability of Data and Materials

The analyzed datasets generated during the study are available from the corresponding author on reasonable request.

Author Contributions

ZL and BL designed the research study; LWZ performed the research; HF collected and analyzed the data. HF has been involved in drafting the manuscript and all authors have been involved in revising it critically for important intellectual content. All authors gave final approval of the version to be published. All authors have participated sufficiently in the work to take public responsibility for appropriate portions of the content and agreed to be accountable for all aspects of the work in ensuring that questions related to its accuracy or integrity.

Ethics Approval and Consent to Participate

Not applicable.

Acknowledgment

Not applicable.

Funding

This work was supported by the Beijing Municipal Natural Science Foundation - Daxing Innovation Joint Fund (L246033).

Conflict of Interest

The authors declare no conflict of interest.

References

[1] Sun H, Saeedi P, Karuranga S, Pinkepank M, Ogurtsova K, Duncan BB, et al. IDF Diabetes Atlas: Global, regional and country-level diabetes prevalence estimates for 2021 and projections for 2045. Diabetes Research and Clinical Practice. 2022; 183: 109119. https://doi.org/10.1016/j.diabres.2021.109119

[2] Li Y, Liu Y, Liu S, Gao M, Wang W, Chen K, et al. Diabetic vascular diseases: molecular mechanisms and therapeutic strategies. Signal Transduction and Targeted Therapy. 2023; 8: 152. https://doi.org/10.1038/s41392-023-01400-z

[3] Hasheminasabgorji E, Jha JC. Dyslipidemia, Diabetes and Atherosclerosis: Role of Inflammation and ROS-Redox-Sensitive Factors. Biomedicines. 2021; 9: 1602. https://doi.org/10.3390/biomedicines9111602

[4] Karthikesh MS, Wu S, Singh R, Paulus Y, Wang X, Yang X. Effect of Photo-Mediated Ultrasound Therapy on Nitric Oxide and Prostacyclin from Endothelial Cells. Applied Sciences (Basel, Switzerland). 2022; 12: 2617. https://doi.org/10.3390/app12052617

[5] Sun D, Chen S, Li S, Wang N, Zhang S, Xu L, et al. Enhancement of glycolysis-dependent DNA repair regulated by FOXO1 knockdown via PFKFB3 attenuates hyperglycemia-induced endothelial oxidative stress injury. Redox Biology. 2023; 59: 102589. https://doi.org/10.1016/j.redox.2022.102589

[6] Wang M, Li Y, Li S, Lv J. Endothelial Dysfunction and Diabetic Cardiomyopathy. Frontiers in Endocrinology. 2022; 13: 851941. https://doi.org/10.3389/fendo.2022.851941

[7] Yan X, Su Y, Fan X, Chen H, Lu Z, Liu Z, et al. Liraglutide Improves the Angiogenic Capability of EPC and Promotes Ischemic Angiogenesis in Mice under Diabetic Conditions through an Nrf2-Dependent Mechanism. Cells. 2022; 11: 3821. https://doi.org/10.3390/cells11233821

[8] Salemkour Y, Lenoir O. Endothelial Autophagy Dysregulation in Diabetes. Cells. 2023; 12: 947. https://doi.org/10.3390/cells12060947

[9] Hu Z, Wu J, Qin L, Jin H, Cao Y, Zhao Y. IGFBP7 down-regulation or overexpression effect on bovine preadipocyte differentiation. Animal Biotechnology. 2021; 32: 21–30. https://doi.org/10.1080/10495398.2019.1642906

[10] Anderlová K, Cinkajzlová A, Šimják P, Kloučková J, Kratochvílová H, Lacinová Z, et al. Association between gestational diabetes mellitus and bioavailability of insulin-like growth factors and role of their binding proteins. Growth Hormone & IGF Research : Official Journal of the Growth Hormone Research Society and the International IGF Research Society. 2022; 67: 101511. https://doi.org/10.1016/j.ghir.2022.101511

[11] Edgerton-Fulton M, Abdul Y, Jamil S, Ergul A. Endothelin-1 (ET-1) contributes to senescence and phenotypic changes in brain pericytes in diabetes-mimicking conditions. Clinical Science (London, England : 1979). 2024; 138: 1009–1022. https://doi.org/10.1042/CS20240328

[12] Wang J, Deng X, Xie Y, Tang J, Zhou Z, Yang F, et al. An Integrated Transcriptome Analysis Reveals IGFBP7 Upregulation in Vasculature in Traumatic Brain Injury. Frontiers in Genetics. 2021; 11: 599834. https://doi.org/10.3389/fgene.2020.599834

[13] Zheng D, Li J, Yan H, Zhang G, Li W, Chu E, et al. Emerging roles of Aurora-A kinase in cancer therapy resistance. Acta Pharmaceutica Sinica. B. 2023; 13: 2826–2843. https://doi.org/10.1016/j.apsb.2023.03.013

[14] Li P, Chen T, Kuang P, Liu F, Li Z, Liu F, et al. Aurora-A/FOXO3A/SKP2 axis promotes tumor progression in clear cell renal cell carcinoma and dual-targeting Aurora-A/SKP2 shows synthetic lethality. Cell Death & Disease. 2022; 13: 606. https://doi.org/10.1038/s41419-022-04973-9

[15] Zhang B, Zhu C, Chan ASC, Lu G. Discovery of a first-in-class Aurora A covalent inhibitor for the treatment of triple negative breast cancer. European Journal of Medicinal Chemistry. 2023; 256: 115457. https://doi.org/10.1016/j.ejmech.2023.115457

[16] Bai T, Li M, Liu Y, Qiao Z, Zhang X, Wang Y, et al. The promotion action of AURKA on post-ischemic angiogenesis in diabetes-related limb ischemia. Molecular Medicine (Cambridge, Mass.). 2023; 29: 39. https://doi.org/10.1186/s10020-023-00635-4

[17] Yi J, Gao ZF. MicroRNA-9-5p promotes angiogenesis but inhibits apoptosis and inflammation of high glucose-induced injury in human umbilical vascular endothelial cells by targeting CXCR4. International Journal of Biological Macromolecules. 2019; 130: 1–9. https://doi.org/10.1016/j.ijbiomac.2019.02.003

[18] Ma H, He S, Yang T, Lu S, Wang X, Yue K, et al. Possible mechanism of Chinese patent Kugan granules against influenza infection: inducing interferon I and suppressing inflammation. Guidelines and Standards of Chinese Medicine. 2025; 3: 155–164. https://doi.org/10.1097/gscm.0000000000000058

[19] Ma CX, Ma XN, Guan CH, Li YD, Mauricio D, Fu SB. Cardiovascular disease in type 2 diabetes mellitus: progress toward personalized management. Cardiovascular Diabetology. 2022; 21: 74. https://doi.org/10.1186/s12933-022-01516-6

[20] Schallmoser S, Zueger T, Kraus M, Saar-Tsechansky M, Stettler C, Feuerriegel S. Machine Learning for Predicting Micro- and Macrovascular Complications in Individuals With Prediabetes or Diabetes: Retrospective Cohort Study. Journal of Medical Internet Research. 2023; 25: e42181. https://doi.org/10.2196/42181

[21] Liu Y, Lyons CJ, Ayu C, O'Brien T. Enhancing endothelial colony-forming cells for treating diabetic vascular complications: challenges and clinical prospects. Frontiers in Endocrinology. 2024; 15: 1396794. https://doi.org/10.3389/fendo.2024.1396794

[22] Tamura K, Hashimoto K, Suzuki K, Yoshie M, Kutsukake M, Sakurai T. Insulin-like growth factor binding protein-7 (IGFBP7) blocks vascular endothelial cell growth factor (VEGF)-induced angiogenesis in human vascular endothelial cells. European Journal of Pharmacology. 2009; 610: 61–67. https://doi.org/10.1016/j.ejphar.2009.01.045

[23] Ding F, Wu H, Han X, Jiang X, Xiao Y, Tu Y, et al. The miR-148/152 family contributes to angiogenesis of human pluripotent stem cell- derived endothelial cells by inhibiting MEOX2. Molecular Therapy. Nucleic Acids. 2023; 32: 582–593. https://doi.org/10.1016/j.omtn.2023.04.020

[24] Fang J, Chang X. Celastrol inhibits the proliferation and angiogenesis of high glucose-induced human retinal endothelial cells. Biomedical Engineering Online. 2021; 20: 65. https://doi.org/10.1186/s12938-021-00904-5